Paf1 and Ctr9 subcomplex formation is essential for Paf1 complex assembly and functional regulation

Xie et al.

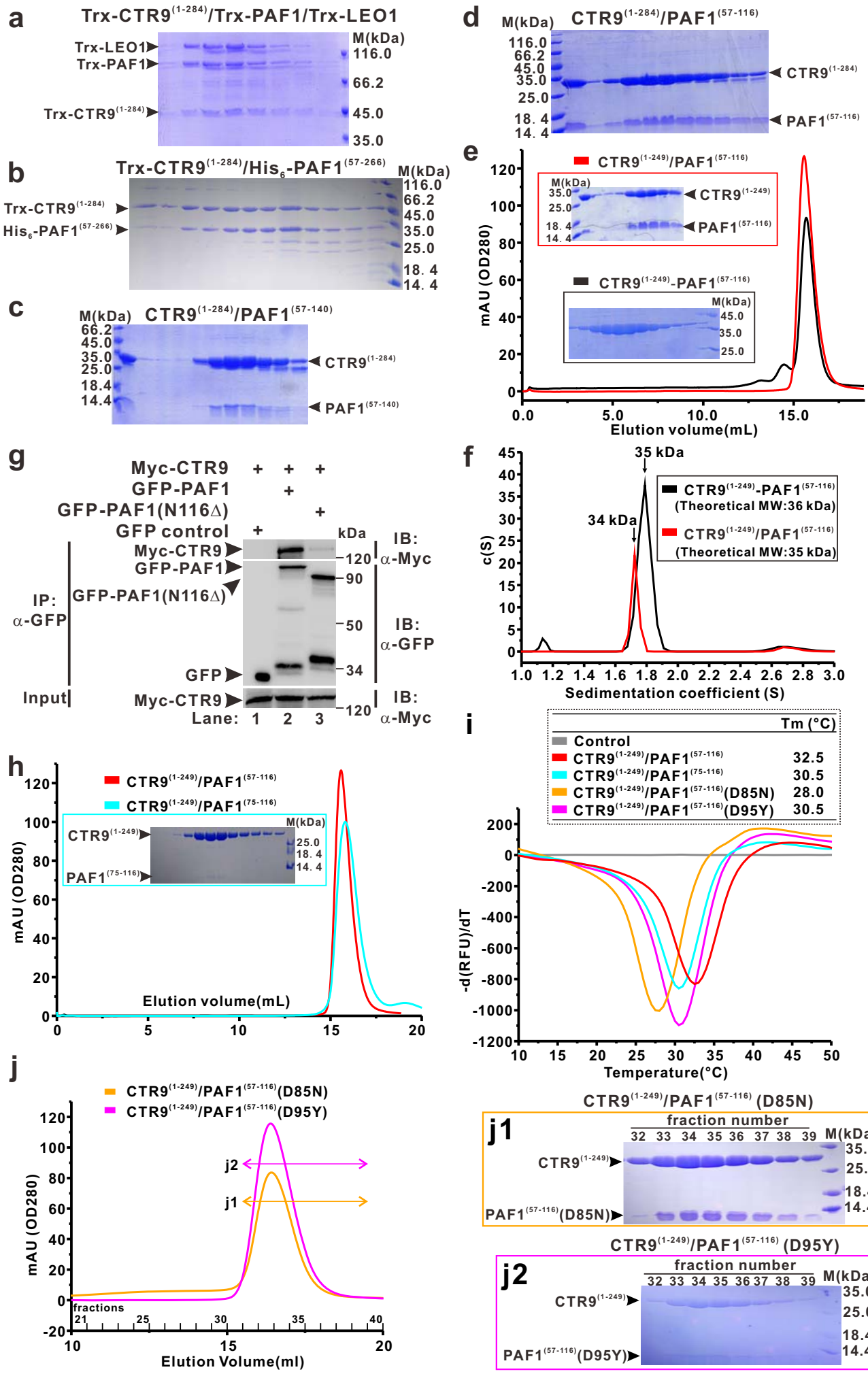
a
Trx-CTR9(1-284)/Trx-PAF1/Trx-LEO1
Trx-LEO1
Trx-PAF1
Trx-CTR9(1-284)
M(kDa)
116.0
66.2
45.0
35.0
b
Trx-CTR9(1-284)/His6-PAF1(57-266)
Trx-CTR9(1-284)
His6-PAF1(57-266)
M(kDa)
116.0
66.2
45.0
35.0
25.0
18. 4
14. 4
c
M(kDa)
CTR9(1-284)/PAF1(57-140)
66.2
45.0
35.0
25.0
18.4
14.4
CTR9(1-284)
PAF1(57-140)
d
M(kDa)
CTR9(1-284)/PAF1(57-116)
116.0
66.2
45.0
35.0
25.0
18. 4
14. 4
CTR9(1-284)
PAF1(57-116)
e
CTR9(1-249)/PAF1(57-116)
M(kDa)
35.0
25.0
18. 4
14. 4
CTR9(1-249)
PAF1(57-116)
CTR9(1-249)-PAF1(57-116)
M(kDa)
45.0
35.0
25.0
mAU (OD280)
120
100
80
60
40
20
0
0.0
5.0
10.0
15.0
Elution volume(mL)
f
35 kDa
34 kDa
CTR9(1-249)-PAF1(57-116)
(Theoretical MW:36 kDa)
CTR9(1-249)/PAF1(57-116)
(Theoretical MW:35 kDa)
c(S)
45
40
35
30
25
20
15
10
5
0
1.0 1.2 1.4 1.6 1.8 2.0 2.2 2.4 2.6 2.8 3.0
Sedimentation coefficient (S)
g
Myc-CTR9 + + +
GFP-PAF1 +
GFP-PAF1(N116Δ) +
GFP control +
kDa
IB:
α-Myc
Myc-CTR9
GFP-PAF1
GFP-PAF1(N116Δ)
120
90
50
34
IP:
α-GFP
IB:
α-GFP
GFP
Input
Myc-CTR9
120
IB:
α-Myc
Lane: 1 2 3
h
CTR9(1-249)/PAF1(57-116)
CTR9(1-249)/PAF1(75-116)
CTR9(1-249)
PAF1(75-116)
M(kDa)
25.0
18. 4
14. 4
mAU (OD280)
120
100
80
60
40
20
0
0
5
10
15
20
Elution volume(mL)
i
Tm (°C)
Control
CTR9(1-249)/PAF1(57-116) 32.5
CTR9(1-249)/PAF1(75-116) 30.5
CTR9(1-249)/PAF1(57-116)(D85N) 28.0
CTR9(1-249)/PAF1(57-116)(D95Y) 30.5
-d(RFU)/dT
200
0
-200
-400
-600
-800
-1000
-1200
10 15 20 25 30 35 40 45 50
Temperature(°C)
j
CTR9(1-249)/PAF1(57-116)(D85N)
CTR9(1-249)/PAF1(57-116)(D95Y)
mAU (OD280)
120
100
80
60
40
20
0
-20
j2
j1
fractions
21
25
30
35
40
10
15
20
Elution Volume(ml)
CTR9(1-249)/PAF1(57-116) (D85N)
j1
fraction number
32 33 34 35 36 37 38 39
M(kDa)
35.0
25.0
18.4
14.4
CTR9(1-249)
PAF1(57-116)(D85N)
CTR9(1-249)/PAF1(57-116) (D95Y)
j2
fraction number
32 33 34 35 36 37 38 39
M(kDa)
35.0
25.0
18.4
14.4
CTR9(1-249)
PAF1(57-116)(D95Y)

Supplementary Figure 1. Human CTR9/PAF1 subcomplex adopt heterodimer with a 1:1 stoichiometry. (**a-e**) SDS-PAGE of various human CTR9/PAF1 recombinant proteins by co-expression after gel filtration. For clarity, analytical gel filtration profiles are not shown, except two separate chains of $CTR9^{(1-249)}$/$PAF1^{(57-116)}$ complex protein and the single chain fusion of $CTR9^{(1-249)}$-$PAF1^{(57-116)}$ protein. "/" denotes protein complex with separate chains, while "-" denotes protein in a single-chain fusion (**e**). (**f**) The molecular weights of the purified proteins were measured by analytical ultracentrifugation sedimentation velocity (SV). c(s) distributions from the SV runs for the $CTR9^{(1-249)}$-$PAF1^{(57-116)}$ (1.4 mg/ml, black line) and $CTR9^{(1-249)}$/$PAF1^{(57-116)}$ (0.5 mg/ml, red line). (**g**) The N-terminal fragment amino acids 1-116 of PAF1 is essential for the interaction between full-length CTR9 and PAF1. Extracts were prepared from HEK293T cells transfected with various combinations of plasmids, as indicated. The bottom panel shows 3% of the Myc fusion proteins for each IP. (**h** and **j**) Analytical gel filtration profiles and SDS-PAGEs of $CTR9^{(1-249)}$/$PAF1^{(57-116)}$ (red line in **h**), $CTR9^{(1-249)}$/$PAF1^{(75-116)}$ (cyan line and insert in **h**), $CTR9^{(1-249)}$/$PAF1^{(57-116)}$(D85N) (**j** and **j1**) and $CTR9^{(1-249)}$/$PAF1^{(57-116)}$(D95Y) (**j** and **j2**). Those fractions shown in correspondent gels are indicated by a two-way arrow. (**i**) Differential scanning fluorimetry-based thermal denaturation assay showing the temperature-dependent denaturation profiles of $CTR9^{(1-249)}$/$PAF1^{(75-116)}$ and $CTR9^{(1-249)}$/$PAF1^{(57-116)}$ WT or mutants. Uncropped gels are shown in Supplementary Fig. 8.

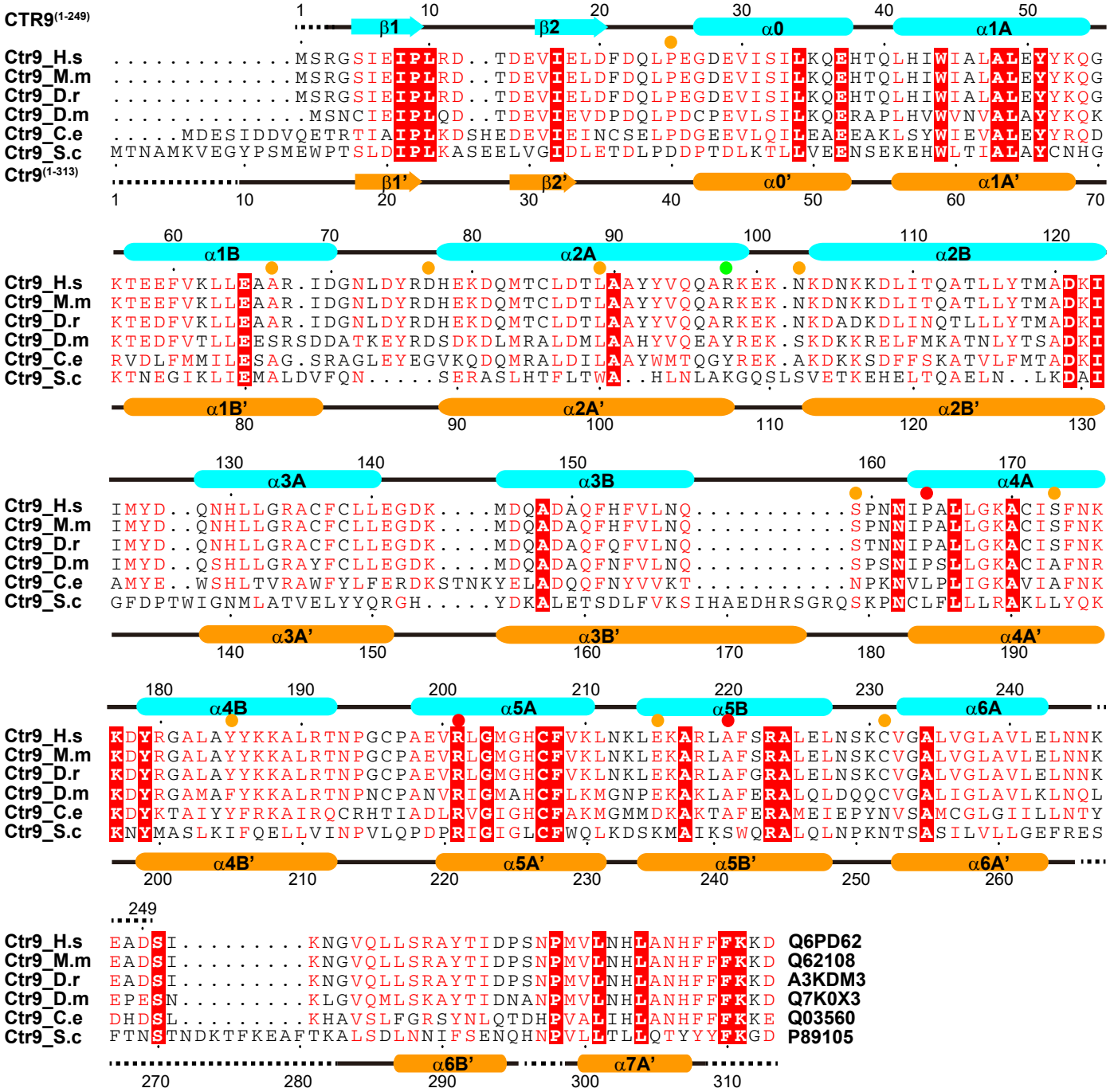
CTR9(1-249)
Ctr9(1-313)
β1
β2
α0
α1A
β1'
β2'
α0'
α1A'
α1B
α2A
α2B
α1B'
α2A'
α2B'
α3A
α3B
α4A
α3A'
α3B'
α4A'
α4B
α5A
α5B
α6A
α4B'
α5A'
α5B'
α6A'
α6B'
α7A'
Ctr9_H.s
Ctr9_M.m
Ctr9_D.r
Ctr9_D.m
Ctr9_C.e
Ctr9_S.c
Q6PD62
Q62108
A3KDM3
Q7K0X3
Q03560
P89105

Supplementary Figure 2. Structure-based sequence alignment of CTR9 from different species. In this alignment, the secondary structures of human CTR9 and yeast Ctr9 are shown at the top and bottom, respectively, according to the crystal structures of $CTR9^{(1-249)}$-$PAF1^{(57-116)}$ and $Ctr9^{(1-313)}$-$Paf1^{(34-103)}$, and conserved residues are shaded in red. The disease-associated amino acids substitutions P164S, R201C, or A220T (Category 1 shown in Fig. **3a**), P25L, A67T D77V, L89F, N102K, S159F, S173F, Y185C, E215K, or C231F (Category 2 shown in Supplementary Table 2), and R98W (Category 3 shown in Fig. **3a**) are indicated with red, orange , and green spheres, respectively. The GenBank numbers are shown at the end of each alignment.

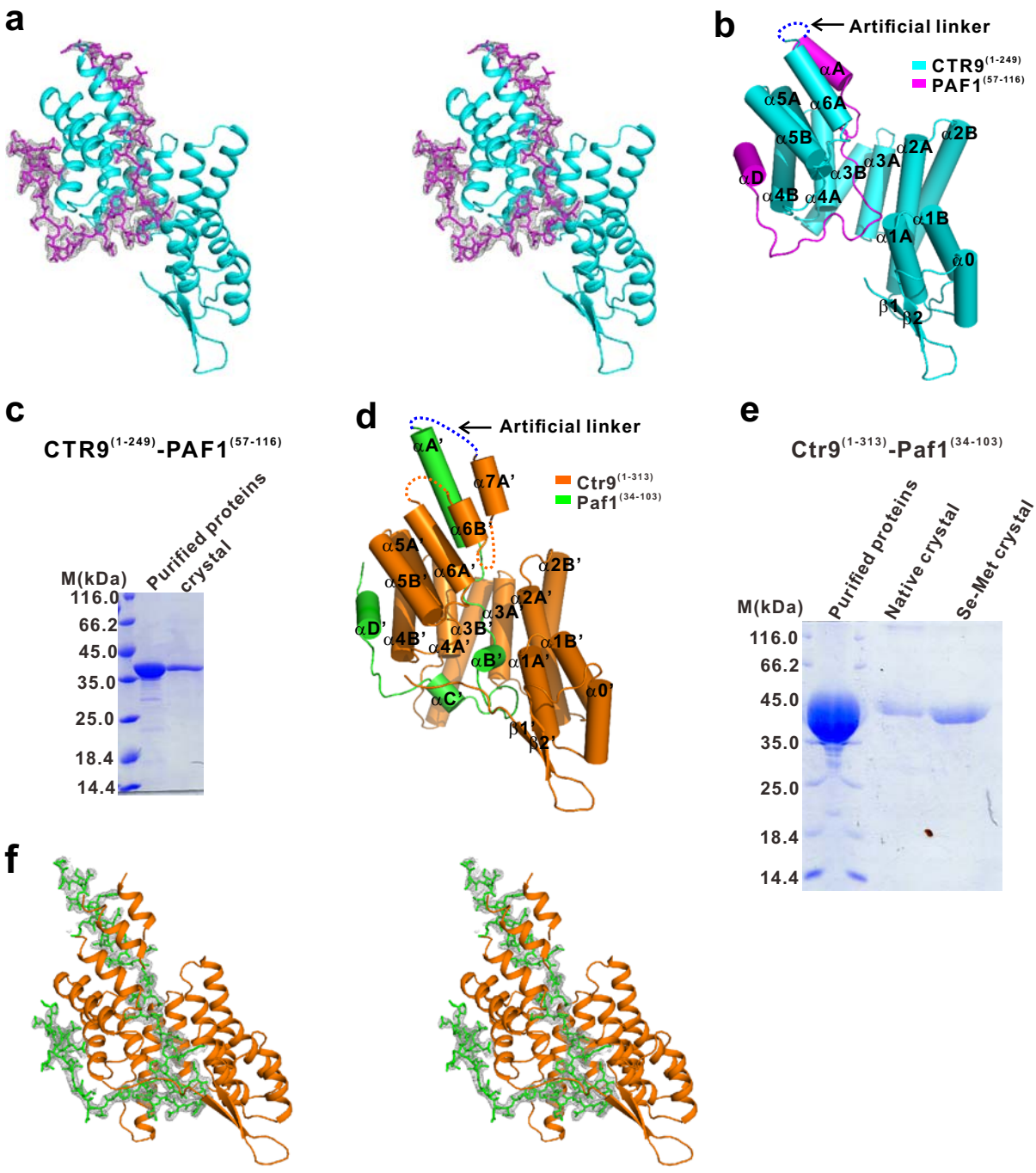
a
b
Artificial linker
CTR9(1-249)
PAF1(57-116)
αA
α5A
α6A
α5B
α2B
α2A
α3A
αD
α3B
α4B
α4A
α1B
α1A
α0
β1
β2
c
CTR9(1-249)-PAF1(57-116)
Purified proteins
crystal
M(kDa)
116.0
66.2
45.0
35.0
25.0
18.4
14.4
d
Artificial linker
αA'
α7A'
Ctr9(1-313)
Paf1(34-103)
α6B'
α5A'
α5B'
α6A'
α2B'
α2A'
α3A'
αD'
α3B'
α4B'
α4A'
α1B'
αB'
α1A'
α0'
αC'
β1'
β2'
e
Ctr9(1-313)-Paf1(34-103)
Purified proteins
Native crystal
Se-Met crystal
M(kDa)
116.0
66.2
45.0
35.0
25.0
18.4
14.4
f

Supplementary Figure 3. Comparison of purified and crystallized proteins. (**a** and **f**) Stereo images of the omit maps for the CTR9/PAF1 heteodimer (**a**) and the Ctr9/Paf1 heterodimer (**f**) contoured at 1.0 σ. (**b** and **d**) Cartoon representations of the overall structure of the single chain fusion of the CTR9 (cyan)/PAF1 (magenta) heterodimer (**b**) and the Ctr9 (orange)/Paf1 (green) heterodimer (**d**). (**c** and **e**) SDS-PAGEs of the Purified $CTR9^{(1-249)}$-$PAF1^{(57-116)}$ and the $CTR9^{(1-249)}$-$PAF1^{(57-116)}$ proteins dissolved from crystals are shown (**c**), and the Purified $Ctr9^{(1-313)}$-$Paf1^{(34-103)}$ and the $Ctr9^{(1-313)}$-$Paf1^{(34-103)}$ proteins dissolved from native or Se-Met crystals are shown (**e**). The crystals were transferred into mother liquor, washed three times and finally dissolved into 10 μl buffer (20 mM HEPES, pH 7.5, 150 mM NaCl, 1 mM EDTA, and 1 mM DTT). All solutions were loaded onto a 15% SDS-PAGE gel.

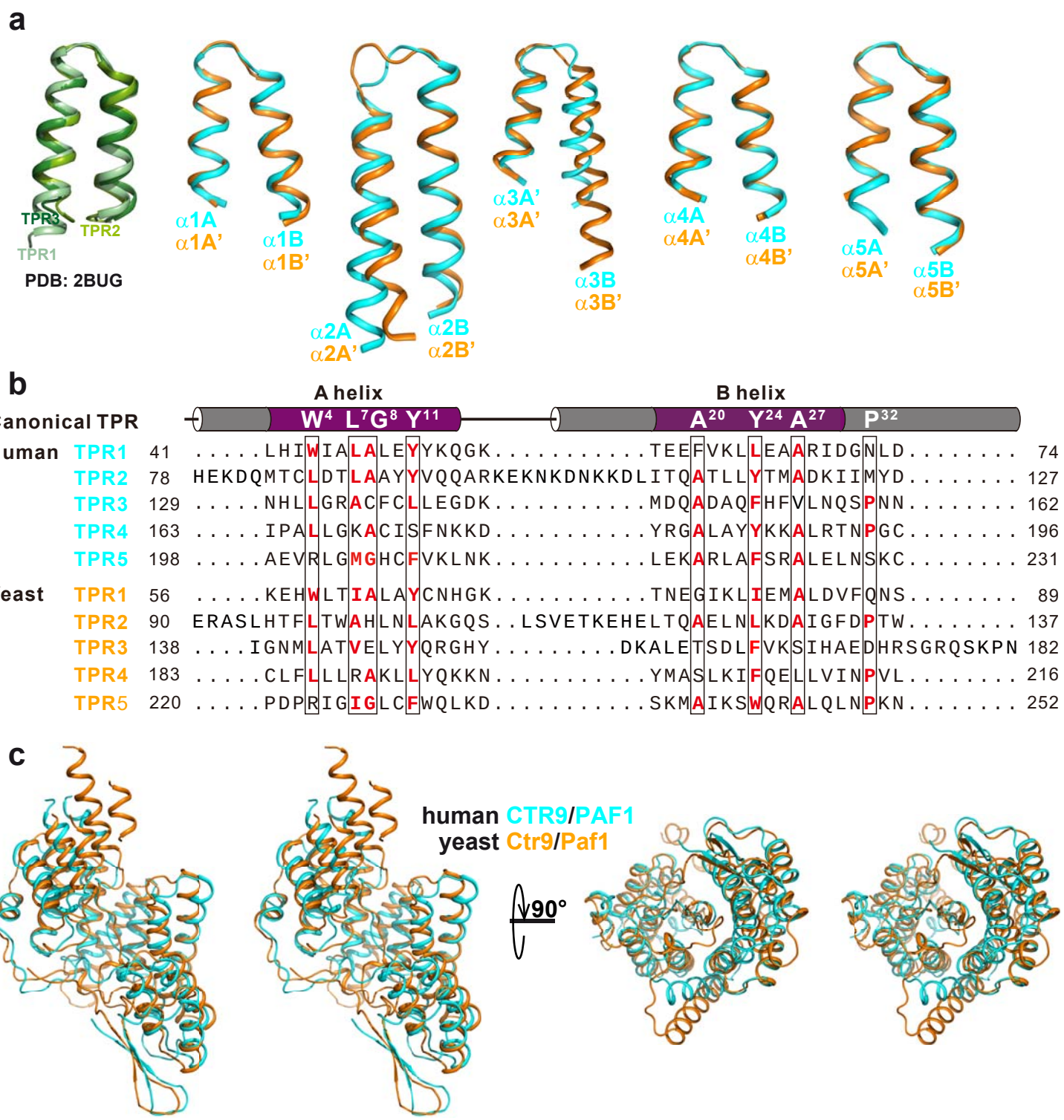
a
TPR3
TPR2
TPR1
PDB: 2BUG
α1A
α1A'
α1B
α1B'
α2A
α2A'
α2B
α2B'
α3A'
α3A'
α3B
α3B'
α4A
α4A'
α4B
α4B'
α5A
α5A'
α5B
α5B'
b
A helix
B helix
Canonical TPR
W4 L7G8 Y11
A20 Y24 A27
P32
Human TPR1 41 .....LHIWIALALEYYKQGK..........TEEFVKLLEAARIDGNLD..... 74
TPR2 78 HEKDQMTCLDTLAAYYVQQARKEKNKDNKKDLITQATLLYTMADKIIMYD..... 127
TPR3 129 .....NHLLGRACFCLLEGDK..........MDQADAQFHFVLNQSPNN..... 162
TPR4 163 .....IPALLGKACISFNKKD..........YRGALAYYKKALRTNPGC..... 196
TPR5 198 .....AEVRLGMGHCFVKLNK..........LEKARLAFSRALELNSKC..... 231
Yeast TPR1 56 .....KEHWLTIALAYCNHGK..........TNEGIKLIEMALDVFQNS..... 89
TPR2 90 ERASLHTFLTWAHLNLAKGQS..LSVETKEHELTQAELNLKDAIGFDPTW..... 137
TPR3 138 ....IGNMLATVELYYQRGHY.........DKALETSDLFVKSIHAEDHRSGRQSKPN 182
TPR4 183 .....CLFLLLRAKLLYQKKN..........YMASLKIFQELLVINPVL..... 216
TPR5 220 .....PDPRIGIGLCFWQLKD..........SKMAIKSWQRALQLNPKN..... 252
c
human CTR9/PAF1
yeast Ctr9/Paf1
90°

Supplementary Figure 4. Human CTR9/PAF1 and yeast Ctr9/Paf1 subcomplexes contain either canonical or atypical TPR motifs and have a similar heterodimeric structure. (**a**) Five TPR motifs of Ctr9 are compared with the canonical TPR fold of the Ppp5 protein. The motifs from human CTR9 and yeast Ctr9 are colored cyan and orange, respectively. (**b**) Structure-based sequence alignment of all 10 TPRs in human CTR9 and yeast Ctr9. The canonical TPR sequence is shown at the top cylinder (Lotus purple) and the conserved residues of Ctr9 are shaded in red. (**c**) Superimposition of the structures of the human CTR9/PAF1 (cyan) heterodimer and the yeast Ctr9/Paf1 (orange) heterodimer.

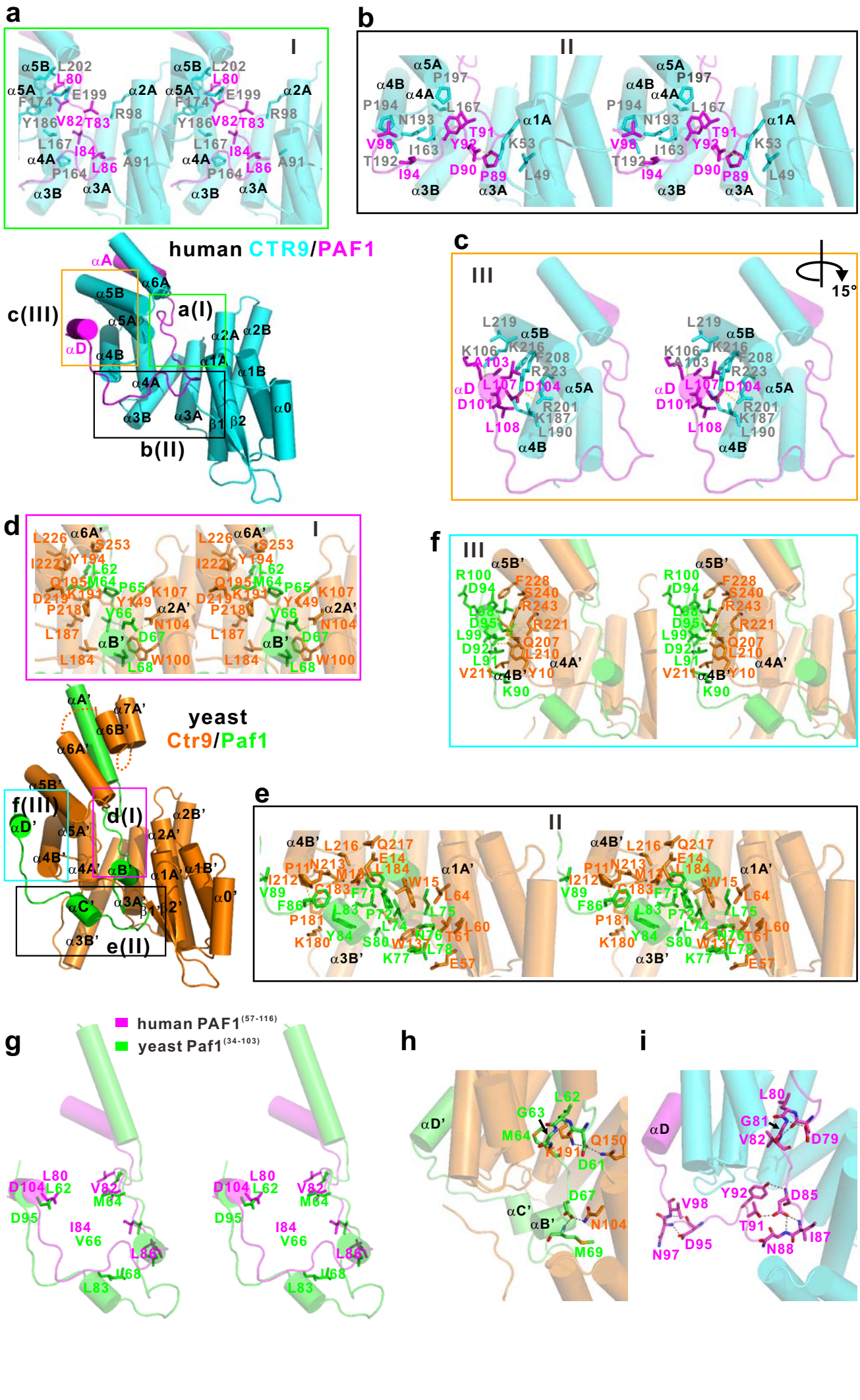
a
I
α5B L202 L80
α5A F174 E199 α2A
Y186 V82 T83 R98
L167 I84
α4A P164 L86 A91
α3B α3A
b
II
α5A P197
α4B α4A
P194 L167
N193 α1A
V98 T91
T192 I163 Y92 K53
I94 D90 P89 L49
α3B α3A
human CTR9/PAF1
αA
α6A
α5B
c(III)
α5A
a(I)
αD
α4B
α2A α2B
α1A
α1B
α4A
α0
α3B α3A β1 β2
b(II)
c
III
15°
L219 α5B
K106 K216
A103 F208
R223
αD L107 D104 α5A
D101 R201
K187
L108 L190
α4B
d
I
L226 α6A' S253
I222 Y194
L62
Q195 M64 P65
D219 K191 K107
Y149
P218 V66 α2A'
N104
L187 αB' D67
L184 W100
L68
f
III
α5B'
R100 F228
D94 S240
R243
D95 R221
L99 Q207
D92 L210
L91 α4A'
V211 α4B' Y10
K90
yeast
Ctr9/Paf1
αA'
α7A'
α6B'
α6A'
α5B'
f(III)
αD'
d(I)
α5A'
α2B'
α2A'
α4B'
α4A'
αB'
α1A'
α1B'
αC'
α3A'
β1' β2'
α0'
α3B'
e(II)
e
II
α4B' L216 Q217
E14
P11 N213
I212 M12 L184 α1A'
V89 W15
C183 F71 L64
F86 L83 P72 L75
P181 L74 L60
Y84 N76 T61
K180 S80 W13 L78
α3B' K77 E57
g
human PAF1(57-116)
yeast Paf1(34-103)
L80
D104 L62 V82
M64
D95
I84
V66
L86
U68
L83
h
αD'
L62
G63
M64 Q150
K191
D61
D67
αC'
αB'
N104
M69
i
αD
L80
G81
V82 D79
Y92 D85
V98
T91
D95 I87
N97 N88

Supplementary Figure 5. The interaction interface of the human CTR9/PAF1 and yeast Ctr9/Paf1 heterodimers. (**a**-**b**) The CTR9$^{(1-249)}$/PAF1$^{(57-116)}$ interface is divided into three regions corresponding to the CTR9 TPR1-5 concave channel/N-terminal loop of PAF1 (**a**), the side of the TPR1-5/C-terminal loop of PAF1 (**b**), and the convex surface of the TPR4-5/αD helix of PAF1 (**c**). (**d**-**f**) The Ctr9$^{(1-313)}$/Paf1$^{(34-103)}$ interface is divided into three regions corresponding to the Ctr9 TPR1-5 concave channel/N-terminal loop of Paf1 (**d**), the side of the TPR1-5/C-terminal loop of Paf1 (**e**), and the convex surface of the TPR4-5/αD' helix of Paf1 (**f**). The interaction details between CTR9 and PAF1 (**a**-**c**) or between Ctr9 and Paf1 (**d**-**f**) in the three regions are shown in stereo view. The side chain of the residues involved in the interactions are drown in the stick model. Charge-charge and hydrogen bonding interactions are highlighted by dashed yellow lines. (**g**) A stereo view of the superimposition of the hook-fold structures of PAF1$^{(57-116)}$ and Paf1$^{(34-103)}$. PAF1 and Paf1 are colored magenta and green, respectively. (**h** and **i**) The highly conserved residues are important for yeast Ctr9/Paf1 (**h**) and human CTR9/PAF1 (**i**) complexes formation. For clarify, only residues involved in hydrogen bonding are shown in (**h**) and (**i**), and the side chain are drawn in the stick model. Hydrogen bonding interactions are highlighted by dashed grey lines.

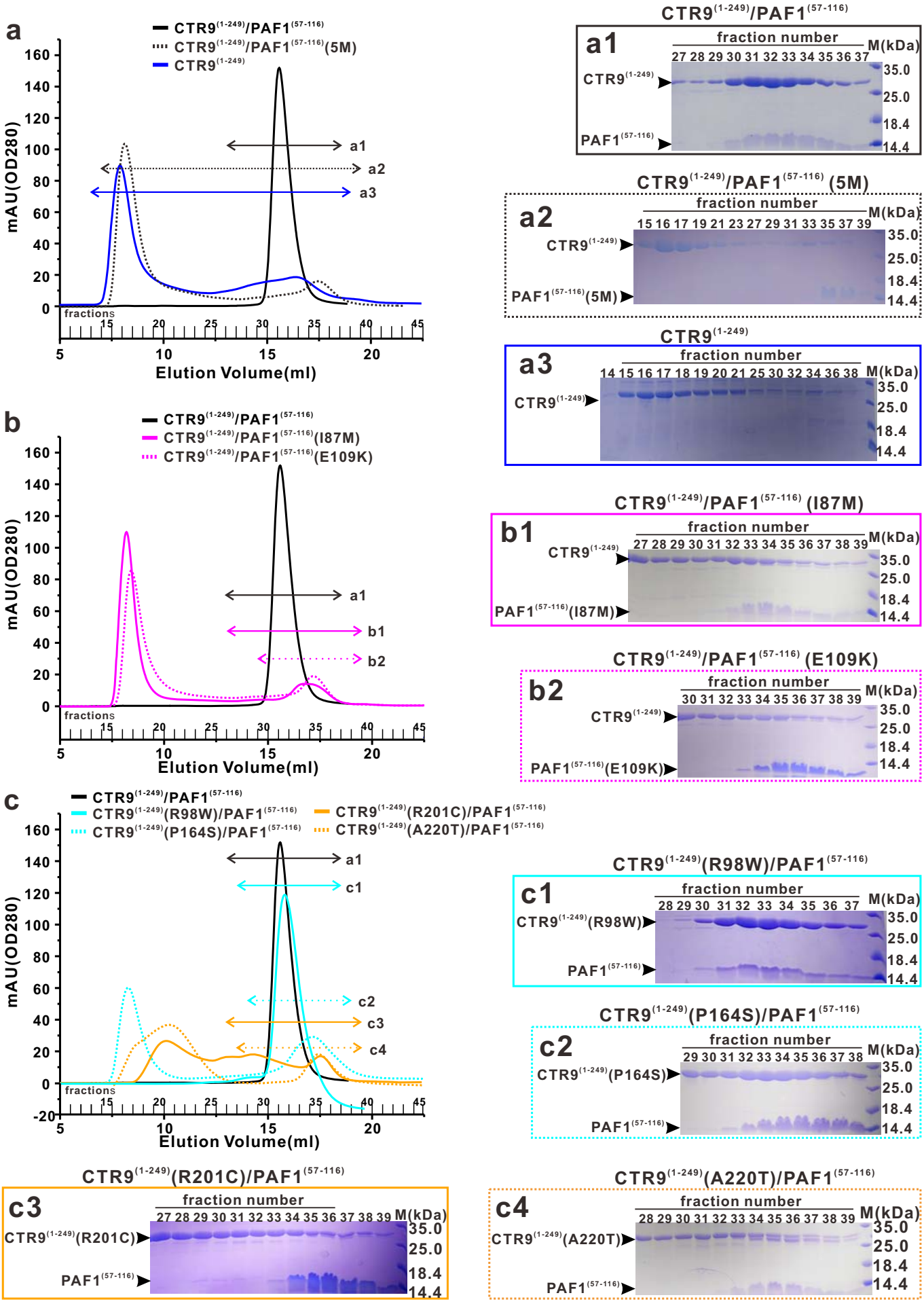
a
CTR9(1-249)/PAF1(57-116)
CTR9(1-249)/PAF1(57-116)(5M)
CTR9(1-249)
mAU(OD280)
fractions
Elution Volume(ml)
a1
a2
a3
b
CTR9(1-249)/PAF1(57-116)
CTR9(1-249)/PAF1(57-116)(I87M)
CTR9(1-249)/PAF1(57-116)(E109K)
b1
b2
c
CTR9(1-249)/PAF1(57-116)
CTR9(1-249)(R98W)/PAF1(57-116)
CTR9(1-249)(P164S)/PAF1(57-116)
CTR9(1-249)(R201C)/PAF1(57-116)
CTR9(1-249)(A220T)/PAF1(57-116)
c1
c2
c3
c4
fraction number
M(kDa)
35.0
25.0
18.4
14.4

Supplementary Figure 6. Disease-associated amino acid substitutions abolish the interactions between CTR9$^{(1-249)}$ and PAF1$^{(57-116)}$. (**a**-**c**) Analytical gel filtration profiles and SDS-PAGEs of CTR9$^{(1-249)}$/PAF1$^{(57-116)}$ (**a** and **a1**), CTR9$^{(1-249)}$/PAF1$^{(57-116)}$(5M) (**a** and **a2**), CTR9$^{(1-249)}$ (**a** and **a3**), CTR9$^{(1-249)}$/PAF1$^{(57-116)}$(I87M) (**b** and **b1**), CTR9$^{(1-249)}$/PAF1$^{(57-116)}$(E109K) (**b** and **b2**), CTR9$^{(1-249)}$(R98W)/PAF1$^{(57-116)}$ (**c** and **c1**), CTR9$^{(1-249)}$(P164S)/PAF1$^{(57-116)}$ (**c** and **c2**), CTR9$^{(1-249)}$(R201C)/PAF1$^{(57-116)}$ (**c** and **c3**), and CTR9$^{(1-249)}$(A220T)/PAF1$^{(57-116)}$ (**c** and **c4**). Those fractions shown in correspondent gels are indicated by a two-way arrow. Uncropped gels are shown in Supplementary Fig. 8.

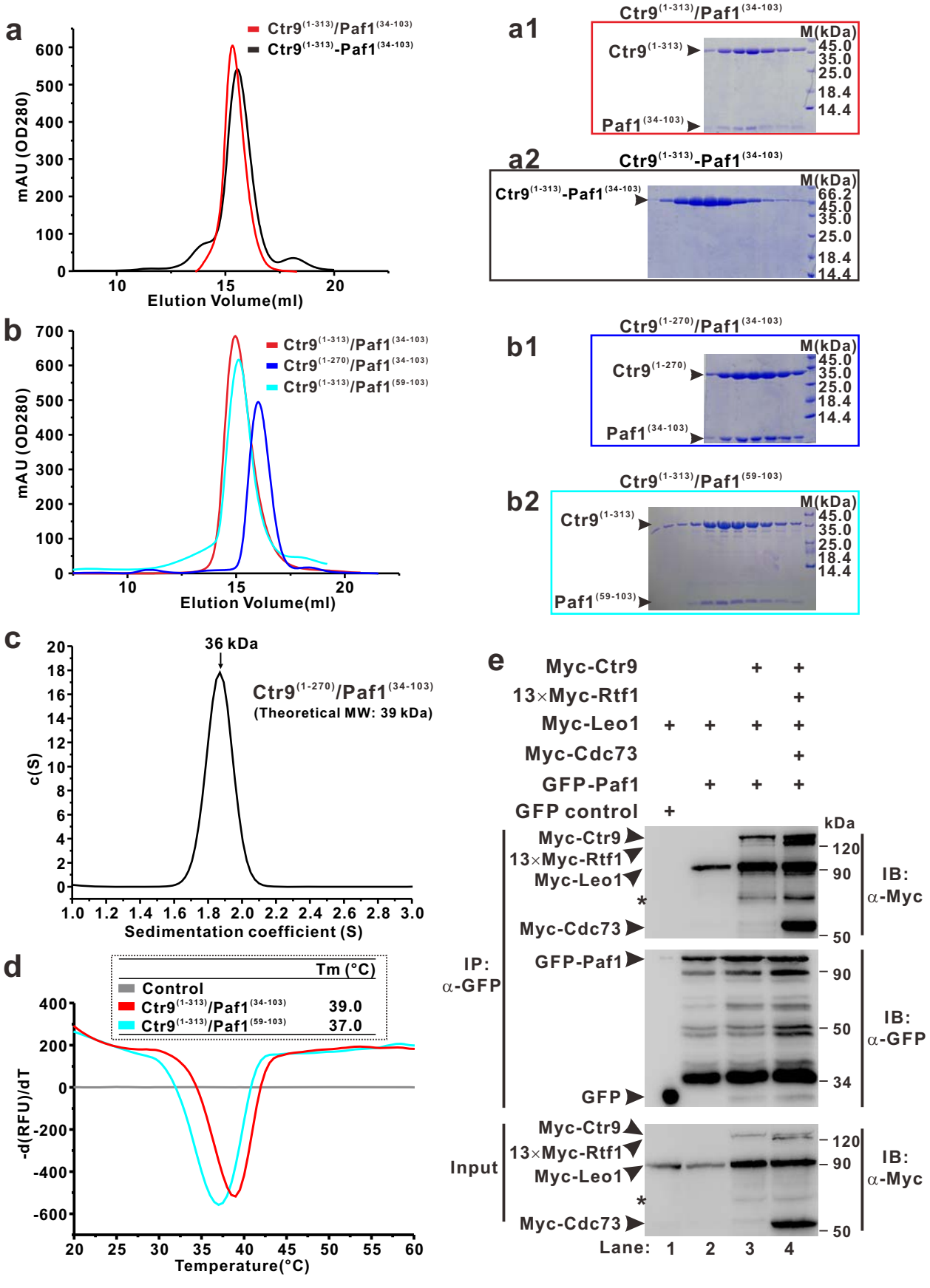
a
Ctr9(1-313)/Paf1(34-103)
Ctr9(1-313)-Paf1(34-103)
mAU (OD280)
Elution Volume(ml)
a1
Ctr9(1-313)/Paf1(34-103)
M(kDa)
Ctr9(1-313)
Paf1(34-103)
a2
Ctr9(1-313)-Paf1(34-103)
b
Ctr9(1-313)/Paf1(34-103)
Ctr9(1-270)/Paf1(34-103)
Ctr9(1-313)/Paf1(59-103)
b1
Ctr9(1-270)/Paf1(34-103)
b2
Ctr9(1-313)/Paf1(59-103)
c
36 kDa
Ctr9(1-270)/Paf1(34-103)
(Theoretical MW: 39 kDa)
c(S)
Sedimentation coefficient (S)
d
Tm (°C)
Control
Ctr9(1-313)/Paf1(34-103) 39.0
Ctr9(1-313)/Paf1(59-103) 37.0
-d(RFU)/dT
Temperature(°C)
e
Myc-Ctr9
13×Myc-Rtf1
Myc-Leo1
Myc-Cdc73
GFP-Paf1
GFP control
kDa
IP: α-GFP
IB: α-Myc
IB: α-GFP
Input
GFP
Lane: 1 2 3 4

Supplementary Figure 7. Yeast Ctr9/Paf1 subcomplexes adopt heterodimers with a 1:1 stoichiometry. (**a** and **b**) Analytical gel filtration profiles and SDS-PAGE of two separate chains of $Ctr9^{(1-313)}$/$Paf1^{(34-103)}$ complex protein (**a** and **a1**) and the single chain fusion of $Ctr9^{(1-313)}$-$Paf1^{(34-103)}$ protein (**a** and **a2**). "/" denotes protein complex with separate chains, while "-" denotes protein in a single-chain fusion. Analytical gel filtration profiles and SDS-PAGEs of $Ctr9^{(1-270)}$/$Paf1^{(34-103)}$ (**b** and **b1**) and $Ctr9^{(1-270)}$/$Paf1^{(59-103)}$ (**b** and **b2**). (**c**) c(s) distributions from the SV run for the $Ctr9^{(1-270)}$/$Paf1^{(34-103)}$ (1 mg/ml). (**d**) Differential scanning fluorimetry-based thermal denaturation assay showing the temperature-dependent denaturation profiles of $Ctr9^{(1-313)}$/$Paf1^{(34-103)}$ (red line) and $Ctr9^{(1-313)}$/$Paf1^{(59-103)}$ (cyan line). (**e**) Co-IP experiments by GFP-tagged yeast Paf1 (GFP-Paf1). Extracts were prepared from HEK293T cells transfected with various combinations of plasmids, as indicated, immunoprecipitated with agarose-conjugated anti-GFP and subsequently immunoblotted with anti-Myc or anti-GFP, as indicated. The top panel shows the IP results. The middle panel represents the IP of GFP and GFP-Paf1. The bottom panel shows 3% input of the Myc fusion proteins used for each IP. The asterisk indicate the degradation of Myc-Ctr9. Uncropped gels and blots are shown in Supplementary Fig. 8.

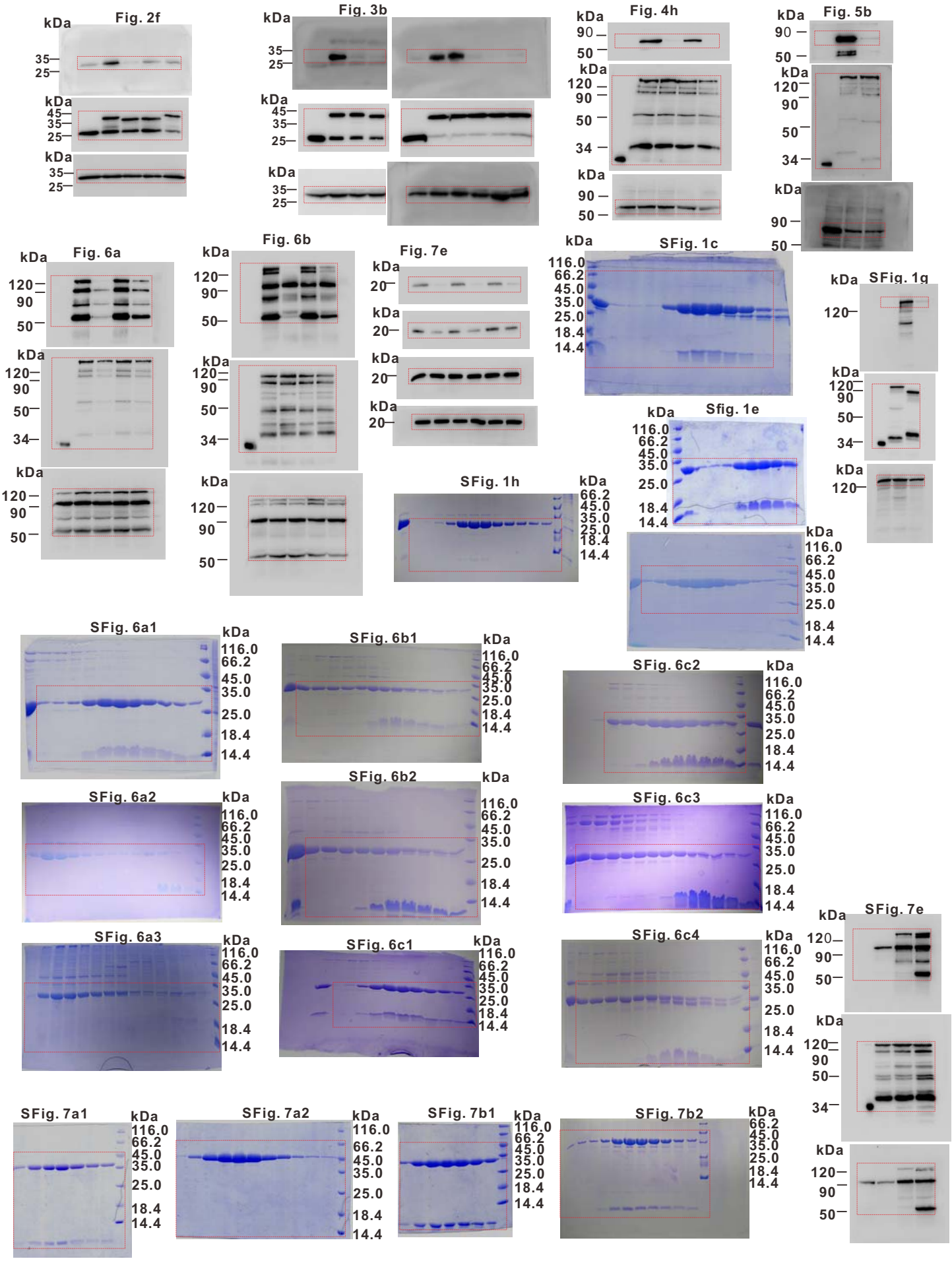

Supplementary Figure 8. Full uncropped figures of western blots and SDS-PAGE gels. Cropped regions are indicated with rectangles as appropriate.

Supplementary Table 1. Data collection and refinement statistics

	Ctr9-Paf1 Se-Met	CTR9-PAF1 Se-Met	CTR9-PAF1 Native
Data collection			
Space group	***P***3221	***P***3112	***P***3112
Cell dimensions			
a, *b*, *c* (Å)	95.95, 95.95, 115.50	82.55, 82.55, 145.54	82.42, 82.42, 145.66
α, β, γ (°)	90, 90, 120	90, 90, 120	90, 90, 120
Resolution (Å)	50.00-2.53 (2.62-2.53) [a]	50.00-2.83 (2.88-2.83) [a]	50.00-2.53 (2.57-2.53) [a]
R_{merge} (%)	4.7 (85.8)	7.3 (67.0)	6.7 (63.2)
$I / \sigma I$	29.2 (2.0)	38.8 (4.0)	28.9 (4.0)
Completeness (%)	99.8 (99.9)	100.0 (99.6)	100.0 (100.0)
Redundancy	5.5 (5.5)	19.7(16.6)	9.9 (10.1)
Refinement			
Resolution (Å)	47.98-2.53		41.21-2.53
No. reflections	35,677		17,815
R_{work} / R_{free}	19.39/24.30		20.18/24.02
No. atoms			
Protein	2,739		2,276
Ligand/ion	3		0
Water	85		103
B-factors			
Protein	47.6		55.7
Ligand/ion	53.5		
Water	39.7		44.9
R.m.s. deviations			
Bond lengths (Å)	0.008		0.009
Bond angles (°)	0.984		1.078

[a] Values in parentheses are for highest-resolution shell.

Supplementary Table 2. Disease-associated mutations in human CTR9

Mutation type	Mutation (Amino acid)
Missence	L10F, E15G, L19I, P25L, Q36R, I43V, A46D, A48V, L63V, A67T, D74H, D77V, L89F, R98W, N102K, D108V, T118A, D121N, Y126C, N129I, H153Y, N157S, S159F, P164S, K169N, S173F, Y185C, K188N, R191H, A198T, R201C, K213T, E215K, A220T, A224S, E226K, C231F, V232M, S250F, S267N, L272W, A276E, V288F, H294Y, M304K, E320G, Y329C, F344C, E376K, G382S, A386T, G399C, H400Y, K402E, D426N, A437T, P450T, L454F, N456D, A459V, G468W, R480S, R480C, A494T, A494S, A494P, A494V, A509V, R525L, E526K, Y534C, R536H, E556A, W568L, G572D, G572V, N573H, W581C, P583H, S596F, G608S, Q613K, R620Q, K624N, R627H, R631H, R631C, K637R, R641K, K645M, N646K, L657V, H659P, R664C, R667C, T677S, A678T, D682V, A688V, A700T, Y704C, Y704D, H714D, V720I, Y722C, A747T, D750N, L764F, D771N, A782V, A789V, Y792N, L796F, V799A, V799L, G800E, D806H, S818F, L820V, R830Q, R830W, R832H, D835Y, E838Q, R839Q, R839W, E846Q, K849N, R853M, L857P, Q860H, R864H, K872N, L874P, R878Q, R878W, E883K, L889I, M890T, F891C, R903G, R910H, R910C, S911C, S911F, E916D, D924Y, D926G, E948D, R961I, G966R, K982Q, R984Q, R985C, P986T, K993R, R999C, P1002L, S1003L, K1007R, S1015L, D1018H, D1022N, L1026H, K1027R, S1059F, N1062S, G1067D, E1069K, G1071S, R1075K, R1099Q, R1080W, P1090S, S1097Y, E1105K, R1122H, S1143Y, N1157I, S1161L, S1165L, D1173N
Nonsense	G27*, Q391*, R394*, E515*, E526*, W553*, Q629*, G654*, G800*, R1077*
Frameshift deletion	T57fs*5, K107fs*96, L475fs*63, V673fs*13, R903fs*102, D923fs*1
Frameshift insertion	L24fs*6 , L368Ffs*6
In-frame deletion	R962delR

Various disease-associated mutations in CTR9 were listed, based on the data extracted from the COSMIC database (http://cancer.sanger.ac.uk/cosmic). A total of 38 missense mutations were located in 38 residues of CTR9$^{(1\text{-}249)}$. These 38 mutations were divided into three categories. The three categories were named as interface, folding, and others, and amino acid substitutions in each category were colored in red, orange, and green, respectively. Only mutations used in this study were shown in Fig. 3a.

Supplementary Table 3. Disease-associated mutations in human PAF1

Mutation type	Mutation (Amino acid)
Missence	R11W, R11L, S38I, D54N, H70Q, K71R, H72N, H72R, H72Q, D73H, D73V, L74I, L74R, T76S, D85N, L86F, I87M, D95N, D95Y, E105D, E109K, A125T, K133N, T134I, E149K, E167K, I176L, P201L, E203D, M250V, D251N, G254R, F261S, E266K, T267M, R271Q, R273Q, E277K, D285N, W297L, N301H, G306D, G318C, R331C, R335H, R336Q, S343L, A347T, R354W, M356T, E358K, K359T, R367W, R367Q, P376L, E412Q, R420W, R420Q, K431R, K431N, E438K, E441K, R445Q, E469K, D470N, R471S, Q475L, D481A, G489A, R492W, S495N, A519V, D522N, A526D, D527N, D527H, D531N
Nonsense	E25*, G28*, W130*, R132*, R198*, E469*, G472*
Frameshift deletion	T76fs*24, S174fs*48, K230fs*11, Q475fs*>57, G485fs*>47
Frameshift insertion	G401fs*>134, G408fs*>125
In-frame deletion	F313delF, E399delE, K406delK, A519_A526delAASDSS...

Various disease-associated mutations in PAF1 were listed, based on the data extracted from the COSMIC database (http://cancer.sanger.ac.uk/cosmic). A total of 17 missense mutations were located in 12 residues of $PAF^{(57\text{-}116)}$. These 17 mutations were divided into three categories. The three categories were named as interface, folding, and others, and amino acid substitutions in each category were colored in red, orange, and green, respectively. Only mutations used in this study were shown in Fig. 3a.

Supplementary Table 4. Yeast strains used in this study.

Strain name	Genotype	Reference
SEY6210	*MATalpha his3D200 leu2–3,112 lys2–801 trp1-D901 ura3–52 suc2-D9 GAL+*	[1]
YXY01	SEY6210 *URA3 LEU2*	This study
YXY02	SEY6210 *paf1::URA3*	This study
YXY03	SEY6210 *paf1::URA3 pP1k-PAF1::LEU2*	This study
YXY04	SEY6210 *paf1::URA3 pP1k-PAF1(4S)::LEU2*	This study
YXY05	SEY6210 *paf1::URA3 pP1k-PAF1(L83S)::LEU2*	This study
YXY06	SEY6210 *paf1::URA3 pP1k-PAF1(D95K)::LEU2*	This study
P	promoter	

Supplementary Reference:

1. Robinson JS, Klionsky DJ, Banta LM, Emr SD. Protein sorting in Saccharomyces cerevisiae: isolation of mutants defective in the delivery and processing of multiple vacuolar hydrolases. *Mol. Cell. Biol.* **8**, 4936-4948 (1988).